Journal of Nano- and Electronic Physics
Vol. **12** No 2, 02009(4pp) (2020)

Журнал нано- та електронної фізики
Том **12** № 2, 02009(4cc) (2020)

Investigating the Effect of Sintering Treatment on Structural and Magnetic Properties of Fe_3O_4 Nanoparticles

I.A. Shaikh*, A.V. Raval, D.V. Shah

Applied Physics Department, SVNIT, Surat, 395007 Gujrat, India

(Received 12 February 2020; revised manuscript received 09 April 2020; published online 25 April 2020)

The magnetite Fe_3O_4 nanoparticles with a size range of 8-9 nm were synthesis by the chemical co-precipitation of ferrous chloride, ferric chloride and NaOH as reducing agent with some modifications in the reported methods. The synthesized magnetic nanoparticles were heated at different temperature in the range of 250 °C to 850 °C. The effect of heating on structural properties of synthesized sample was studied by X-ray diffraction (XRD) and field effect scanning electron microscope (FESEM). The XRD patterns confirm the formation crystalline phase of Fe_3O_4 nanoparticles. The pattern formation of the nanoparticles was observed upon sintering treatment. Also there was a phase transition from magnetite (Fe_3O_4) to hematite (α-F_2O_3) was observed when the samples was heated above 550 °C. The vibrating sample magnetometer (VSM) was used to study the magnetic properties, hysteresis curve and the saturation magnetisation. The saturation magnetisation decreases as the annealing temperature increases which is attributed to the phase transformation.

Keywords: Magnetic nanoparticles, Sintering, Magnetite, Maghemite, Hematite.

DOI: 10.21272/jnep.12(2).02009 PACS number: 71.20.Be

1. INTRODUCTION

The iron oxide magnetic nanomaterials, magnetite (Fe_3O_4), hematite (α-Fe_2O_3) and maghemite (γ-Fe_2O_3), have gained great interests in the past few years for owing to their fascinating properties, abundance in nature and ease of synthesis. The properties which make it an ideal candidate for the research are the biocompatibility, ease in surface modification and magnetic properties [1]. Further at nanoscale the single magnetic domain induces the superparamagnetism and size dependent properties. The most common applications of magnetic nanomaterials in the field of medicine are drug delivery system (DDS) [2], MRI contrast agent [3] and hyperthermia [4].

Depending on the experimental conditions at the time of synthesis one or more of the iron oxide phases may be formed. This can be avoided by controlling the experimental conditions and ensure the presence of a single-phase as the magnetic properties change with the phase transition. The magnetite, pure black in colour, is oldest iron oxide magnetic material and thermodynamically unstable. When heated in the presence of oxygen it oxidized to hematite, hematite and maghemite at different temperature. This puts limitation in its applications in places where the temperature conditions are much higher than the room temperature [5].

The magnetic properties of the iron oxide nanoparticles depend on the crystal phase transition occurring at different temperature or oxidising condition. The crystal phase transition mainly depends on the particle size, precursors used, conditions, heating rate and sintering time. It was observed that the particle size increased from 6.6 to 37.6 nm by increasing temperature from 50 to 850 °C and therefore the saturation magnetization (Ms) increased from 41.69 to 53.61 emu/g till temperature 550 °C, and then decreased intensively to 0.49 emu/g at 850 °C [6]. The pure magnetic nanoparticles with an average crystallite size of 48 nm when heated at 650 °C the crystallite size of increases with heating temperature and holding time. The nanoparticles gave the highest saturation magnetization 97.99 emu/g, higher than synthesised nanoparticles but the change was not that drastic [7]. The particle size of 8 nm were synthesised by chemical method had decreasing magnetisation from 60 emu/g to 14 emu/gm when heated upto 500 °C [8].

As limited reports are available on the current topic, the behavioural study of magnetic nanoparticles at different temperatures for different sintering time is needed.

The present paper presents the result obtained in the study of sintering effect on Fe_3O_4 nanoparticles when heated in the range of 50 °C to 850 °C for 120 minutes.

2. EXPERIMENTAL

2.1 Synthesis of Fe_3O_4 Nanoparticles

Materials

All chemicals used for the synthesis were AR grade and used without any further purification. Precursors used were ferrous chloride tetrahydrate ($FeCl_2.4H_2O$), ferric chloride hexahydrate ($FeCl_3.6H_2O$) and sodium hydroxide (NaOH).

Synthesis of Fe_3O_4 Nanoparticles

The Fe_3O_4 nanoparticles were synthesized by the chemical co-precipitation of $FeCl_2.4H_2O$ and $FeCl_3.6H_2O$ with molar ratio of 1:2 with NaOH as a reducing agent. Inert atmoshphere was maintained in the reactor by using flow of N_2 gas as the oxidation in the inert atmoshphere will oxidise it to $Fe(OH)_3$. At first, 0.1 M solution of $FeCl_2.4H_2O$ and 0.2 M of $FeCl_3.6H_2O$ in 100 ml deionised water was reduced with 0.8 M of NaOH in 100 ml of deionised water. The NaOH solution was

* israrS_74@yahoo.co.in

added drop wise with the help of addition funnel with pressure equalising tube. The solution was stirred for 3 hours on magnetic stirrer at 300 rpm. The black precipitate was formed which was allowed to settle magnetically overnight. Next day, the supernatant liquid was removed carefully and the precipitate was redispersed in 100 ml water. The process was repeated three times to obtain high purity [9]. The precipitate was dried in an oven at temperature of 50 °C. The sample was crushes to powder with a mortar and pestle.

The chemical reaction can be given as,

$$2FeCl_3 + FeCl_2 + 8NaOH \rightarrow Fe_3O_4(s) + 4H_2O + 8NaCl$$

Upon sintering the crystal phase is changing which is a of oxidation of the Fe_3O_4 nanoparticles, the reaction for it can be written as

$$2Fe_3O_4 + ½O_2 \rightarrow 3(\gamma\text{-}Fe_2O_3) \text{ at } 250\ °C$$

and

$$2Fe_3O_4 + ½\ O_2 \rightarrow 3(\alpha\text{-}Fe_2O_3) \text{ at } 700\ °C$$

Sintering of Fe_3O_4 Nanoparticles

The fine powder was divided into six equal parts and transferred to a crucible. One part is not heated and taken as it is while the second part was placed in the furnace and heated to temperature 250 °C for 120 minutes. The furnace was allowed to cool naturally and when it reached room temperature the sample was removed and used for further characterisations. Similarly, samples were heated to 400, 550, 700, 850 °C [10].

2.2 Characterizations

The structural property of the synthesised nanoparticles were studied by X-ray diffraction (XRD) which was recorded by Rigaku Ultima IV, Japan Xray diffractometer operating at 40 KV-40 mA using CuKα radiation ($\lambda = 1.5406$ Å). The morphology and crystal size was observed by field effect scanning electron microscope (FESEM) (Hitachi S-4800). The magnetic property, hysteresis loop, was studied by a vibrating sample magnetometer (VSM: LakeShore 7309).

3. RESULTS AND DISCUSSION

3.1 Structural and Morphological Analysis

As shown in the Fig. 1, the XRD peaks are seen at angles 30.0°, 36.6°, 43.0°, 53.8°, 57.2°, and 62.9° corresponding to the planes (220), (311), (400), (422), (511) and (440). The peaks are sharp and distinct, revealing excellent crystallinity and homogeneity. The diffraction peaks are matching with reported data indicating the formation of a single phase spinel structure. The average crystallite size in Fe_3O_4 nanoparticles was determined from their XRD patterns using the Debye-Scherrer equation [11],

$$D = \frac{k\lambda}{\beta \cos\theta} \text{ Å}$$

where D is the average crystallite size in Fe_3O_4 nanoparticles, $\lambda = 1.5406$ Å is the wavelength of X-ray, β is the full width of half-maxima (FWHM) of the diffraction line and θ is the Bragg's angle and k is the Scherrer constant (0.9). Gaussian peak fit is used for the best fit on the highest intensity peak. The particle size is calculated by Scherrer formula which varies from 8 to 13 nm with increase in sintering temperature from 50 to 850 °C except for 550 °C at which the particle size is 14 nm.

At 50 °C XRD of Fe_3O_4 is shown in Fig. 1. The observed peaks are at (220), (311), (400), (511) and (440) planes confirming the face centred cubic spinel structure (JCPDS Card No. 19-0629). Upon sintering at 250 and 400 °C, the X-ray diffraction (XRD) peak lines are observed remained same as that of Fe_3O_4. The only variation is slight shift towards higher angles from 35.72° for Fe_3O_4 to 35.80° for γ-Fe_2O_3 (JCPDS Card No. 39-1346). At 550 °C transition from γ-Fe_2O_3 phase to α-Fe_2O_3 phase can be seen. But at temperatures 700 °C and 850 °C peaks corresponding to α-Fe_2O_3 phase can be seen at (012), (104), (110), (113), (024), (116), (018) and (214) (JCPDS Card No. 33-0664) [12]. The morphology and particle size of the synthesised nanoparticles were determined using FESEM. The FESEM images were taken for four samples sintered at different temperature i.e. at 50 °C, 250 °C, 550 °C and 850 °C. The Fig. 2 shows the corresponding images. The FESEM images confirm that the particle are spherical in shape with the size range of 8-14 nm. As the sintering temperature is increased agglomeration and pattern formation can be seen. With the rise in temperature the pattern formation become clear and prominent [13-14].

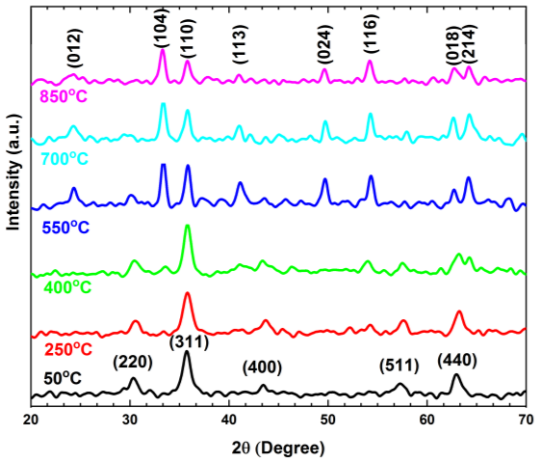

Fig. 1 – XRD of Fe_3O_4 nanoparticles sintered at different temperature

3.2 Magnetic Properties

The room temperature magnetic properties were studies by VSM up to 10000 Oe. The synthesis magnetic Fe_3O_4 nanoparticles exhibit ferromagnetism and superparamagnetic behavior. The Fig. 3 shows the hysteresis curves of nanoparticles before sintering (Fe_3O_4) and after sintering at 250 °C, 550 °C (γ-Fe_2O_3) and 850 °C (α-Fe_2O_3) for 120 minutes. It can be seen from the graph that the magnetic properties of iron oxide nanoparticles change with the phase transition from Fe_3O_4 to α-Fe_2O_3. The Fe_3O_4 nanoparticles have the maximum saturation magnetisation of 43 emu/g, but decreases when heated. For temperature 250 °C and 550 °C the change is not that significant

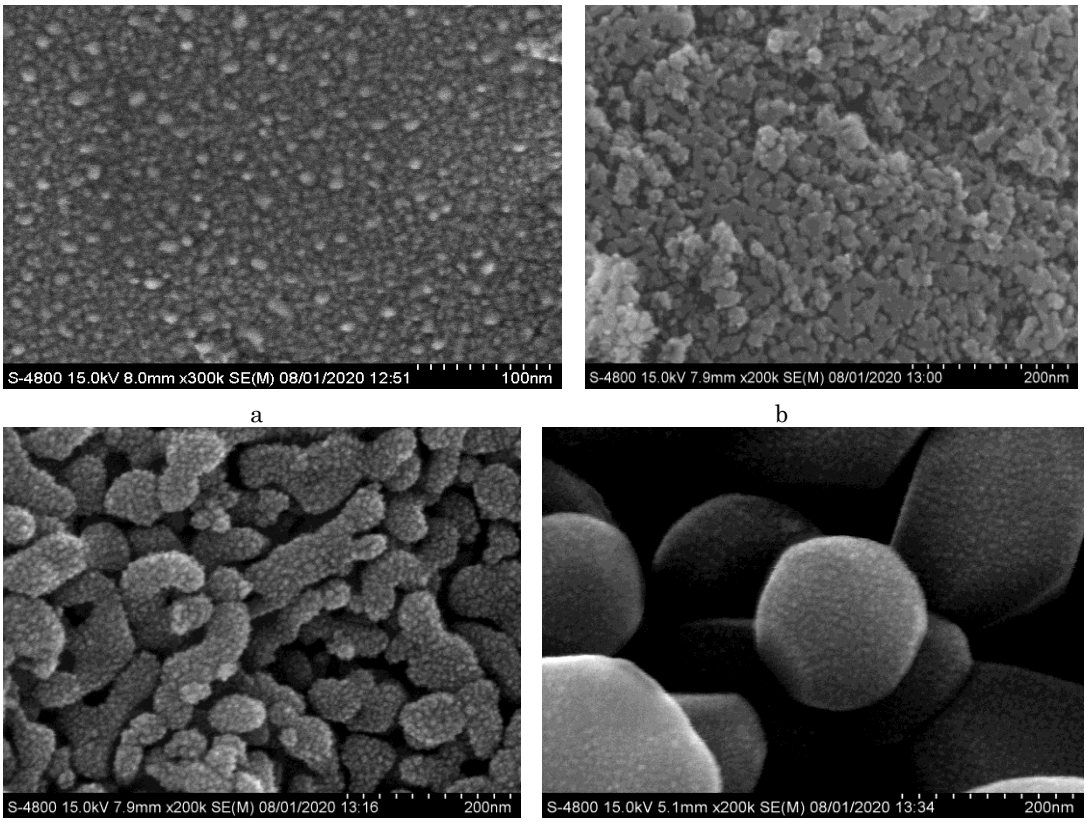

Fig. 2 – FESEM image at $T = 50$ °C before (a) sintering and after sintering at 250 °C (b), 550 °C (c) and 850 °C (d)

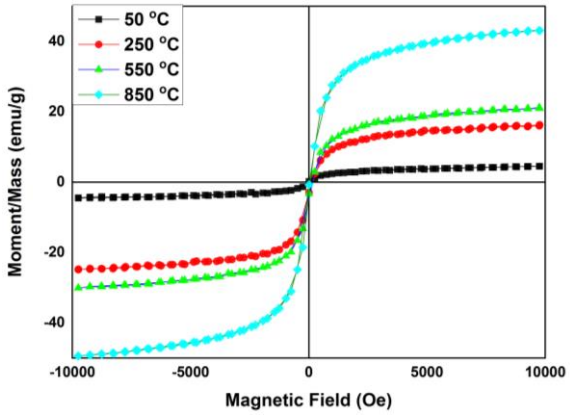

Fig. 3 – VSM at $T = 50$ °C before (a) sintering and after sintering at 250 °C (b), 550 °C (c) and 850 °C (d)

as the loss of magnetism may be compensated by the increase in the particles size to certain extent. But for 850 °C, when the phase is totally transformed to α-Fe_2O_3 phase the saturation magnetisation has reduces to just 4.7 emu/g [15].

4. CONCLUSION

The present study shows that the sintering of magnetic nanoparticles of Fe_3O_4 in air results in the phase transition Fe_3O_4 to γ-Fe_2O_3 to α-Fe_2O_3. This transformation of the phase results in a drop in saturation magnetisation from 43 emu/g to 4.7 emu/g. As the temperature is raised the phase transition happened smoothly giving pure phase at specific temperature and two phases coexist at intermediate temperatures. The crystal morphology changes significantly with sintering temperature. The particle size increases from 8 nm to 13 nm.

REFERENCES

1. Chia-Chang Lin, Jui-Min Ho, Min-Shan Wu, *Powder Technol.* **274**, 441 (2015).
2. Melania Babincova, Peter Babinec Biomed Pap, *Med. Fac. Univ. Palacky. Olomouc. Czech. Repub.* **153 No 4**, 243 (2009).
3. Yong-kang Sun, Ming Ma, Yu Zhang, Ning Gu, *Colloid. Surface A* **245**, 15 (2004).
4. Challa S.S.R. Kumar, Faruq Mohammad, *Adv. Drug Deliv. Rev.* **63**, 789 (2011).
5. I. Abu-Aljarayesh, A. Al-Bayrakdar, S.H. Mahmood, *J. Magn. Magn. Mater.* **123**, 267 (1993).
6. A. Jafari, Shayesteh. S. Farjami, M. Salouti, K. Boustani, *J. Magn. Magn. Mater.* **379**, 305 (2015).
7. Ping Hu, Shengen Zhang, Hua Wang, De'an Pan, Jianjun Tian, Zhi Tang, Alex A. Volinsky, *J. Alloy. Compd.* **509**, 2316 (2011).
8. S.S. Pati, S. Gopinath, G. Panneerselvam, M.P. Antony, John Philip *J. Appl. Phys.* **112**, 054320 (2012).
9. I.A. Shaikh, D.V. Shah, *AIP Conf. Proc.* **2162**, 020113 (2019).
10. I. Kazeminezhad, S. Mosivand, *Acta Phys. Pol. A* **125**, 1210 (2014).
11. N.V. Desai, I.A. Shaikh, K.G. Rawal, D.V. Shah, *AIP Conf. Proc.* **1953**, 030149 (2018).

12. Wei Wu, Zhaohui Wu, Taekyung Yu, Changzhong Jiang, Woo-Sik Kim, *Sci. Technol. Adv. Mater.* **16**, 023501 (2015).
13. Zhang Li-Ying, Dou Yong-Hua, Zhang Ling, Gu Hong-Chen, *Chin. Phy. Lett.* **24**, 483 (2007).
14. T.F. Marinca, H.F. Chicinas, B.V. Neamtu, O. Isnard, P. Pascuta, N. Lupu, G. Stoian, I. Chicinas, *Mater. Chem. Phys.* **171**, 336 (2016).
15. M. Aliahmed, N. Nasiri Moghaddam, *Mater. Sci.-Poland* **31** No 2, 264 (2013).